Tellus (1991), *44A*, 180–196

Antarctic mesocyclone regimes from satellite and conventional data

By MARK FITCH and ANDREW M. CARLETON, *Climate and Meteorology Program, Department of Geography, Indiana University, Bloomington, IN 47405, USA*

(Manuscript received 15 August 1990; in final form 21 May 1991)

ABSTRACT

Mesoscale vortices in the Antarctic, poleward of 50° S, are examined in the synoptic context for the Ross Sea sector (100° E eastward to 80° W) for transition and winter months of 1988, using DMSP (Defense Meteorological Satellite Program) thermal infrared (TIR) images. Mesoscale vortices are classified and tracked and the dominant characteristics, such as life span, speed of movement and preferred geographic locations of formation, are defined and discussed. A "superposed epoch" (compositing) method utilizing 1000 and 500 mb height data identifies the dominant synoptic regimes in which mesoscale vortices tend to develop. This analysis indicates that during active or outbreak periods, a negative thickness anomaly ("cold pool") is located northeast of the Ross Sea, and mesoscale vortices tend to occur on the poleward side of that anomaly. In addition, an enhanced trough-ridge pattern is evident for the Ross Sea sector compared with the composite pattern for inactive, or dearth, periods. The active periods of mesoscale vortices appear to originate from Antarctica, possibly via the persistent katabatic outflows from the ice sheet, rather than from teleconnections to lower latitudes. Analysis of Automatic Weather Station (AWS) data for the Ross Sea region supports this notion, at least for individual cases. Confirmation of these findings for the corresponding months of additional years is continuing.

1. Introduction

Subsynoptic scale vortices that form over the oceans in cold air masses poleward of major fronts during low-sun seasons ("polar air vortices" or "polar lows") have received much attention in Northern Hemisphere studies (Businger and Reed, 1989). These mesoscale vortices (MSVs) occur on relatively small spatial (100–1000 km) and brief temporal (5–48 h) scales and can elude the operational synoptic reporting network. However, heavy rain and snow may accompany these disturbances (e.g., Harrold and Browning, 1969; Monteverdi, 1976; Browning and Hill, 1985). At the same time, MSVs are not unknown over the middle-latitude continents in winter (e.g., Mullen, 1979; Mills and Walsh, 1988). Documentation of the typical synoptic-scale environments in which MSVs evolve is a first step in the accurate prediction of these disturbances and their incorporation into operational prediction models (e.g., Businger, 1985, 1987; Forbes and Lottes, 1985).

Mature mesocyclones display a range of satellite-observed cloud signatures that include the familiar "comma cloud" (Reed, 1979), "spiral-banded" (Rasmussen, 1979, 1981), "merry-go-round" (Zick, 1983) and "boundary-layer front" (Businger and Reed, 1989) configurations (Figs. 1–3). The exact agency for the genesis of MSVs is not entirely understood, although it is widely agreed that they develop either under regions of strong positive vorticity advection (PVA) or in association with the sea ice-ocean margin in higher latitudes (Businger and Reed, 1989). Mesocyclone development in the North Pacific has been ascribed predominantly to baroclinic instability in the initial stages, with subsequent growth sustained by sea-air interactions (e.g., Sardie and Warner, 1985). These conditions are conducive to the genesis of "comma clouds" (e.g., Fig. 1), which occur with particularly high frequency relative to the other types over the North Pacific (e.g., Yarnal and Henderson, 1989a, b).

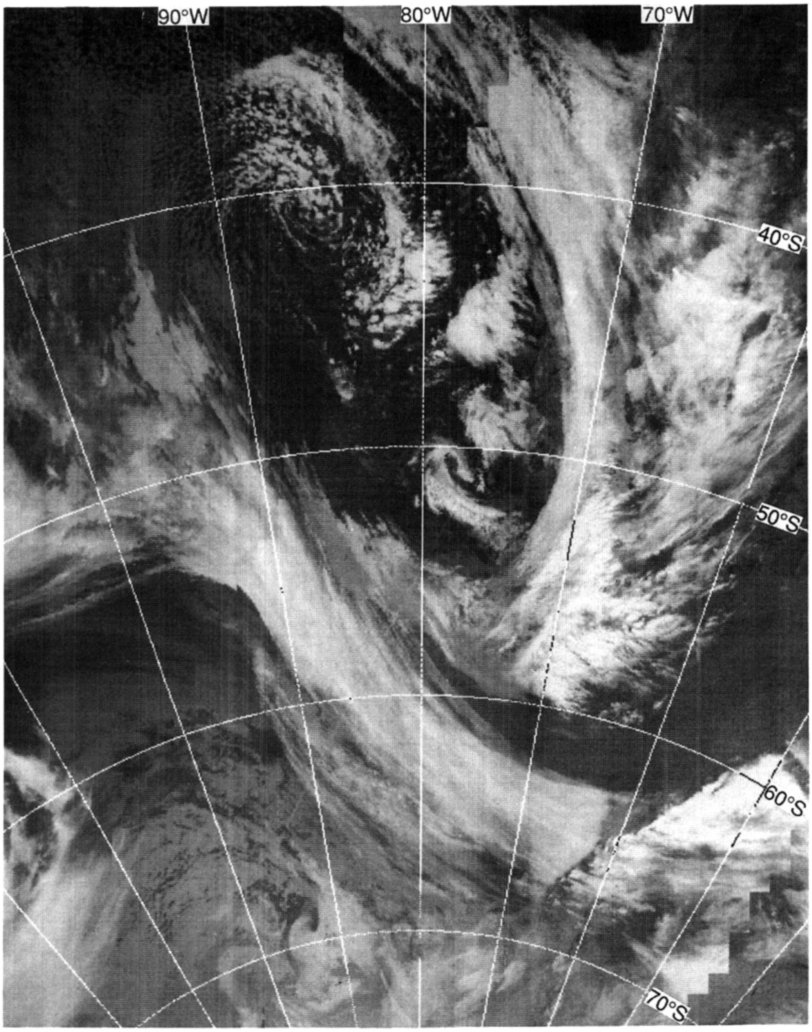

Fig. 1. DMSP TIR 5.4 km resolution image showing several comma cloud systems over a wide range of latitudes to the west and south-west of South America. An Antarctic comma cloud (68° S, 93° W) which has formed in the region of the Bellingshausen Sea, and a middle-latitude comma cloud (52° S, 78° W), are particularly prominent (0055 GMT, 22 July 1989).

In contrast to the baroclinic instability theory of MSV development, thermal instability in an essentially barotropic flow (CISK: Conditional Instability of the Second Kind) may be important in the initiation of spiral-banded MSVs (e.g., Rasmussen, 1979; Økland, 1987). While purely convective CISK-type MSVs are observed on satellite images, particularly over the North Atlantic in winter (Businger and Reed, 1989), recent work (e.g., Shapiro et al., 1987) suggests that at least some degree of baroclinicity is often involved in the initiation of many spiral-banded MSVs. The latter may result from a low-level thermal gradient between the sea-ice or land-ice edge and the ice-free ocean (Businger, 1987). In satellite imagery, this pre-existing feature may be evident as a "boundary-layer front" (e.g., Fig. 2a and 2b). The resulting self-exciting systems are

(a)

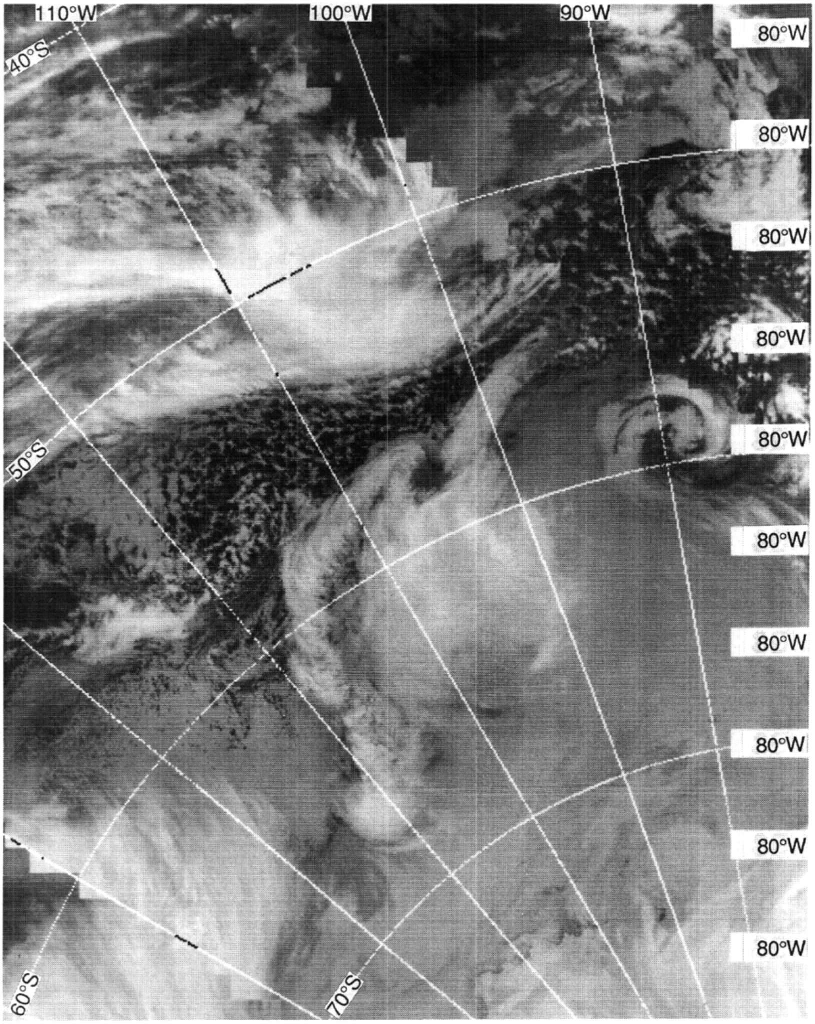

Fig. 2. DMSP TIR sequence (5.4 km resolution) for the south-east South Pacific showing development of a polar air vortex on (a) a "boundary layer front" located just equatorward of the sea ice margin (1212 GMT, 3 October 1988); (b) 3 h later, a spiral vortex with multiple bands is clearly apparent in image center.

often referred to as "Arctic hurricanes", or "true polar lows" (e.g., Rasmussen, 1985; Businger and Reed, 1989; Emanuel and Rotunno, 1989). An example for the Southern Hemisphere appears in Fig. 2b. Favored regions for the development of this type of MSV in the Northern Hemisphere are the Greenland, Norwegian and Barents Seas (Businger and Reed, 1989). Another satelitte-observed environment in which MSVs form is in association with a decaying cold-core synoptic vortex over the ocean (e.g., Fig. 3). This configuration has been described particularly by Zick (1983).

The proliferation of studies of MSVs for the Northern Hemisphere has not been matched in the Southern Hemisphere context. (Witness, for example, the major research effort "The Polar Lows Project", aimed at understanding the dynamics, energetics and climatology of "Arctic hurricanes" over the northern North Atlantic: e.g.,

(b)

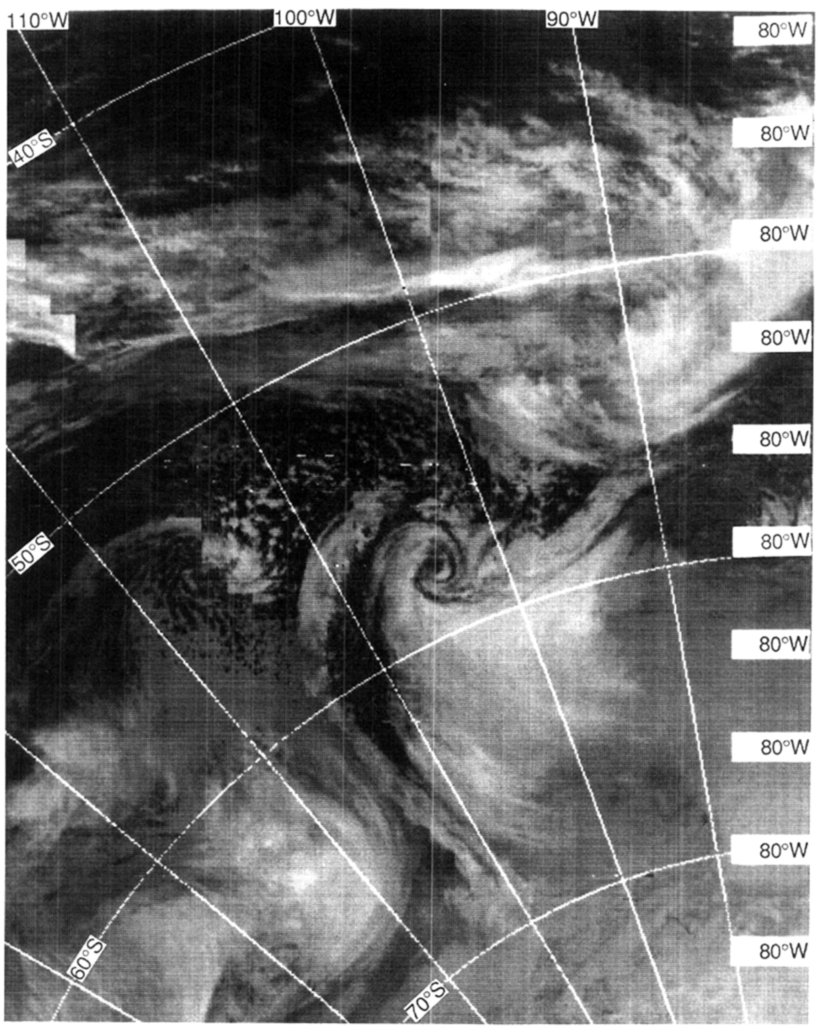

Fig. 2 (cont'd).

Rasmussen and Lystad, 1987; Shapiro et al., 1987.) For example, it has only recently been shown (Carleton and Carpenter, 1989a, 1990) that a corollary to the "Arctic hurricane" also appears to exist in the Antarctic (e.g., Fig. 2b). Although the Northern Hemisphere studies (e.g., Rasmussen, 1981; Shapiro et al., 1987) suggest that MSV "hurricanes" are dominantly warm-cored, there are important geographical differences between the two high-latitude regions that make it unwise to apply Arctic results directly to the Antarctic. These include, for the north-east Atlantic during the winter season, the proximity of relatively warm ocean having strong latitudinal gradients of temperature adjacent to both the sea ice in the north and to the cold Scandinavian land surface in the south. This has no corollary in the Southern Hemisphere. Moreover, the occurrence of strong and persistent katabatic (downslope) winds off the Antarctic ice sheet (Parish and Bromwich, 1987) may be closely connected with mesoscale cyclogenesis in favored regions such as the Ross Sea (Bromwich, 1989), the Amundsen Sea and off the coast of Adelie Land (Parish and Bromwich,

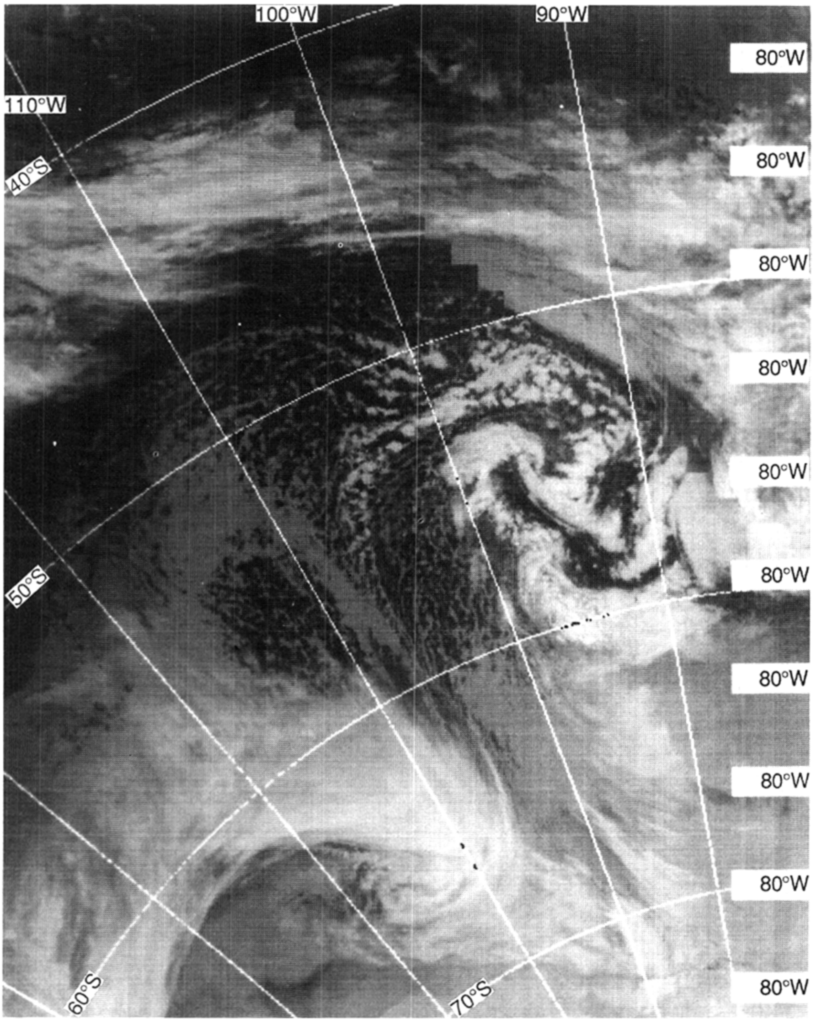

Fig. 3. Portion of a DMSP TIR mosaic (5.4 km resolution) for the south-east Pacific showing multiple polar air vortices developing around an old cyclonic vortex (center right of image)—the "merry-go-round" type. A frontal wave cyclone is located to the south-west (lower center). (1459 GMT, 4 October 1988).

1986). Diagnostic case studies and composite analysis of mesoscale cyclones have been made for limited longitudinal sectors and time periods (Lyons, 1983; Auer, 1986; Sinclair, 1986). These studies have tended to focus on the comma cloud systems that occur predominantly over the open oceans; often well equatorward of the marginal ice zone (MIZ) (e.g., Streten and Troup, 1973; Carleton, 1979). Very little attention has hitherto been paid to mesoscale cyclogenesis over the higher ocean and sea ice latitudes (poleward of about 50° S) of the Antarctic. Yet these systems may be important in the snowfall climatology of coastal regions; particularly in the West Antarctic (Bromwich, 1989). Clearly there is a need to determine the incidence of MSVs over higher southern latitudes.

The present paper presents a synoptic study of MSVs for the half hemisphere centered on the Ross Sea (100° E–80° W), and utilizes satellite and conventional meteorological data for 5 months of 1988 representative of the transition and winter seasons (March, April, June, August and October). Previous studies are contradictory as to the season of maximum frequency of Southern Hemisphere MSVs. For example, Lyons (1983) suggests that a maximum of these systems in the South America sector occurs during the fall and spring. However, satellite studies for the entire hemisphere poleward of 50° S by Carleton and Carpenter (1989a, b, 1990), and comparisons with similar studies for the other seasons (Streten and Troup, 1973), have indicated that the low sun months have the highest occurrences of MSVs. Thus there is a need to resolve this discrepancy.

The availability of DMSP (Defense Meteorological Satellite Program) TIR (thermal infrared) polar orbiter imagery in the official archive is restricted to those months in which low sun conditions preclude the use of the visible channel data over higher latitudes (i.e., from about March through October). The TIR images are required for the analysis of mesocyclone cloud systems since the latter are generally much easier to detect against the background cloud and snow/ice surfaces when compared with the simultaneous visible-band imagery. It should be noted that coverage was good to excellent (twice-daily mosaics available for the majority of days) for all months except March 1988, when there were sizeable temporal gaps in the record. Accordingly, that month is not included in most of the statistics presented in Section 3. This study covers 3 transition months (March, April and October) and 2 winter months (June and August) of 1988 in an effort to:

(1) identify the month(s) of peak occurrence of MSVs (winter versus transition months) and the main characteristics of MSVs. The latter include the favored regions of formation, movement and dissipation, and the typical durations and translation speeds of MSVs;

(2) describe quantitatively the composite synoptic environments in which MSVs form and develop by comparing active, or outbreak, periods with periods of relative quiescence ("inactive");

(3) assess the precursors to MSV outbreaks in the Antarctic context; these include particularly the role of off-ice flows (katabatic winds).

To meet these objectives, we use sets of medium resolution (5.4 km) DMSP twice-daily imagery in conjunction with conventional data. The latter include analyzed charts of the Australian National Meteorological Center, and the tri-hourly records from the extensive network of Automatic Weather Stations (AWSs) in the Ross Sea sector (Keller et al., 1989). Although we present here the results for only one year (1988), the results are at least broadly consistent with similar studies of the synoptic environments of MSVs in the Northern Hemisphere (e.g., Businger, 1985, 1987; Wilhelmsen, 1985; Ese et al., 1988; Forbes and Lottes 1988). They will be checked for consistency in the Southern Hemisphere context by analysis of corresponding months for an additional year (1989) in a subsequent study.

2. Data and their analysis

2.1. DMSP imagery

The use of high or even moderate resolution satellite imagery, in conjunction with observational data, has allowed researchers to study MSVs in the synoptic context (e.g., Mullen, 1979; Forbes and Lottes, 1985; Yarnal and Henderson, 1989a, b; Carleton and Carpenter, 1989a, b, 1990; Heinemann, 1990). The satellite data used in the present study are the medium resolution (5.4 km) TIR images obtained from the polar orbiting DMSP system. The images are computer processed by the US Air Force Global Weather Center (AFGWC) into half-hemispheric mosaics and mapped onto a polar stereographic projection at a scale of 1:30M. The mosaics utilized for the study area (100° E eastward to about 80° W and south of 50° S) are produced twice daily. Availability of the DMSP hard-copy images has become irregular as the USAF prepares to change over to an all digital record.

Each MSV, identified by its small size (minimum size of 1° of latitude: Forbes and Lottes, 1985; Carleton and Carpenter, 1990) and characteristic cloud configuration (e.g., Figs. 1–3), was assigned a unique number for tracking purposes, and all observations of that system from genesis to decay were tabulated. Recorded data on mesocyclones include: the date; the time, given as the equatorial crossing time of the satellite and whether ascending or descending node; location;

dominant cloud-type (cumuliform, stratiform) and cloud height (high-middle, low-middle); vortex signature type (comma cloud, spiral, boundary-layer front, merry-go-round) and stage of development (incipient, mature, dissipating); whether the system continued over more than one satellite mosaic; and other general or special comments. The cloud vortex classification represents commonly recognized signatures of MSVs identified in previous studies (e.g., Businger and Reed, 1989). They are not intended to imply particular physical processes in the absence of corroborating data. We emphasize that the cloud signature types are not necessarily mutually exclusive: the "boundary-layer front" signature may give rise subsequently to either a "comma cloud" or "spiral" MSV; a "merry-go-round" vortex may give rise to multiple comma clouds; and so on. With regard to the "instant occlusion" type, which describes a process, the vortex so designated is considered to be that resulting from the merger of any MSV (spiral, comma) with a pre-existing cloud band (e.g., Carleton, 1985). The data on MSV characteristics are analyzed separately for each of the 5 months, tabulated, and general inferences drawn.

2.2. Conventional data and analysis

Northern Hemisphere studies documenting the synoptic-scale environments in which MSVs evolve have used SLP (sea level pressure) and tropospheric height data in a "superposed epoch" (composite) method of analysis (Businger, 1985, 1987; Ese, et al., 1988). We adopt a broadly similar technique in the present Southern Hemisphere satellite study. In common with the study of Businger (1985) we compute mean 1000 and 500 mb height anomaly maps for each of the identified "active" and "inactive" days. Active (inactive) days are defined as the central day of a series having high (low) occurrences of MSVs for the full study region in a given month. We consider high (low) occurrences to be on the order of greater than 5 (less than 2). These are identified by graphing daily MSV frequencies against time. Table 1 lists the "active" and "inactive" peak days so defined for the four months having good DMSP TIR coverage (April, June, August and October). The data used in this analysis are the daily SLP and 500 mb height maps provided by the Australian Bureau of Meteorology, and the climatological pressure and height data of Taljaard et al. (1969). The latter are based on the period 1956 to 1966.

Table 1. *List of active and inactive days*

	Active	Inactive
April	11th 15 th 19 th	4th 25th
June	3rd 11th 19th	8th 27th
August	22nd 25th 30th	4th 15th
October	11th 21st	9th 15th 24th
Total	11 days	9 days

The anomaly map for active or inactive days for the region (either the 1000 or 500 mb level), is obtained by:

(1) subtracting the daily height field from the climatological monthly mean field;

(2) averaging the anomaly maps so obtained for the month;

(3) Compositing by totally then averaging the monthly anomaly maps across the four months of April, June, August and October.

Since the Taljaard et al. (1969) climatology gives data for the sea-level mean pressure rather than for 1000 mb, the daily pressure anomalies are adjusted with respect to 1000 mb by means of the hydrostatic approximation. Additionally, mean 1000–500 mb thickness anomaly maps are computed separately for the active and inactive composites. This procedure was also used to obtain composite charts 24 h prior to the peak (T_{-24}) of an active or inactive period, as an indicator of antecedent synoptic conditions.

Mesoscale ground surface observations for specific site locations in the Antarctic are available for 29 AWSs (Fig. 4). This network records the air temperature, wind speed, wind direction and air pressure every 3 h. The information from the AWSs is transmitted and received by NOAA polar orbiting satellites. These data are used here to

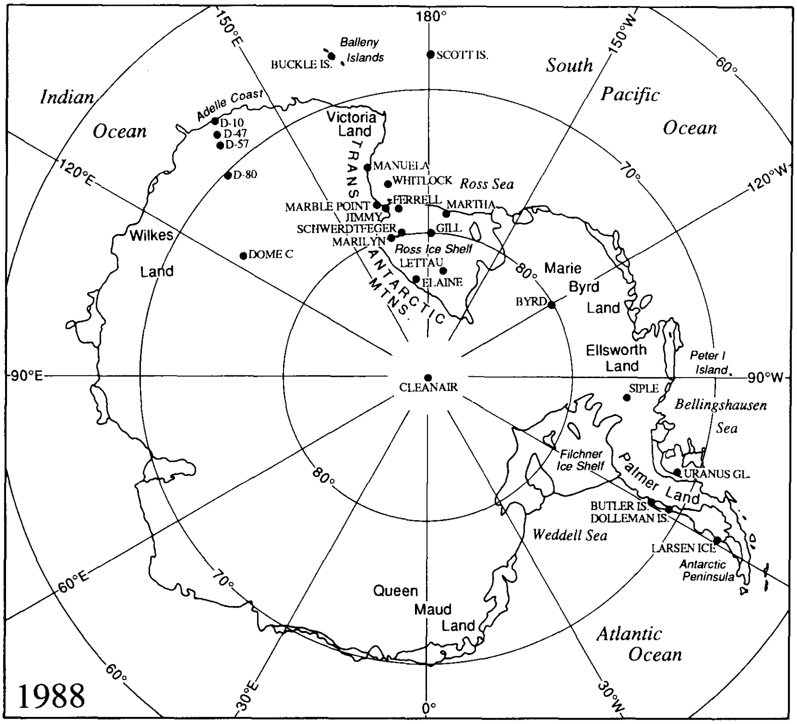

Fig. 4. Map showing location of Antarctic AWSs (Automatic Weather Stations) for 1988, identified by site name (redrawn from Keller et al., 1989).

provide insights into the possible role of the Antarctic ice sheet in the Ross Sea sector in the generation of MSVs.

3. Results and discussion

3.1. Satellite characteristics of Antarctic mesocyclones, 1988

Table 2 shows summary statistics for mesocyclones in the half hemisphere centered on the Ross Sea and south of 50° S for the months of March, April, June, August and October, 1988. In that year the transition months (April and October) show the highest occurrences of mesocyclones when the frequencies are normalized to the number of available images. This result may reflect the stronger temperature gradients in subantarctic latitudes during these months (Schwerdtfeger, 1960).

Based on the broad classification of MSVs according to cloud configuration, statistical distinctions are made between the different signature types (Table 2). The majority of MSV cloud signatures were identified as either "comma" or "spiral-banded" cloud formations (88 %). There were 102 comma and 103 spiral-banded systems in the study period. Of interest is the near 1:1 ratio of these two dominant cloud signatures over the latitudes considered. This contrasts with the broader-scale study for the winter months of 1977–83 by Carleton and Carpenter (1989a, b; 1990), in which the comma clouds outnumbered the spiraliform systems by about 3:1 in subantarctic latitudes. We are not at this time able to explain these different results of the present study compared with those of Carleton and Carpenter (1989a, b, 1990), except perhaps in terms of the highly anomalous nature of the broadscale circulation in 1988 (Climate Monitoring Bulletin Southern Hemisphere, 1988). This question will be pursued further when the data for the subsequent year (1989) have been analyzed. We also find that MSVs may exhibit a signature change between

Table 2. *Mesocyclone statistics from DMSP 5.4 km IR imagery: 1988*

	Month				
	March	April	June	August	October
System raw total[1]:	37	53	46	47	50
System normalized total[2]:	71	62	46	47	67
Single observation[3] (%):	20 (54)	13 (25)	4 (9)	2 (4)	6 (12)
Cyclogenesis Mode:					
Sea ice-ocean margin[4] (%):	8 (22)	22 (41)	20 (43)	16 (34)	15 (30)
Land ice-edge[5] (%):	9 (24)	6 (11)	7 (15)	9 (19)	8 (16)
Other (ocean, ice) (%):	20 (54)	25 (47)	19 (41)	22 (47)	27 (54)
Cyclogenetic Stage:					
Comma cloud (%):	19 (51)	25 (47)	24 (52)	18 (38)	16 (32)
Spiral (%):	16 (43)	24 (45)	18 (39)	19 (40)	26 (52)
"Boundary-layer front" (%):	0 (0)	1 (2)	1 (2)	5 (11)	4 (8)
"Merry-go-round" (%):	1 (3)	2 (4)	2 (4)	2 (4)	3 (6)
"Instant occlusion" (%):	1 (3)	1 (2)	1 (2)	3 (6)	1 (2)
Signature change?[6] (%):	—	10 (25)	7 (17)	9 (20)	6 (14)
Mean Duration (hours):					
Comma cloud	—	26	20	17	18
Spiral	—	17	18	13	22
Mean Speed (m s^{-1}):					
Comma cloud	—	13.0	9.7	15.1	13.3
Spiral	—	14.0	11.9	5.1	13.3

Notes:

[1] For latitudes south of 50° S and longitudes 100° E eastward to 80° W.
[2] Raw total normalized according to number of available images in that month.
[3] A given mesocyclone observed on only one image.
[4,5] Cloud vortex initially observed within $\pm 2.5°$ latitude of the sea-ice or land-ice edge.
[6] Vortex signature changes between first and second observation (e.g., spiral becomes comma) for a system observed on more than one image.

Numbers given in parentheses ( ) are percentages.

sequential images in the initial stages (12% of the systems identified). The fundamental change in cloud signature indicates the operation of complex dynamics during the life-span of MSVs, and which may be common to both comma and spiral systems (Carleton, 1985; Myrberg et al. 1990). The very low frequencies of the boundary-layer front, merry-go-round and instant occlusion signature types (Table 2) indicates primarily the very transient nature of these vortices.

We also considered the duration and speed of MSVs separately for the comma cloud and spiraliform types, for the 4 months in which there were few gaps in the DMSP coverage (Table 2). The approximate mean duration was determined by recording the image time when the MSV was first identified and the time of its final observation. Computation of the speeds used the above information, as well as the change in latitude and longitude of the vortex.

With regard to vortex duration (Table 2), there were no significant differences among the 4 months

(April, June, August, October) for either the comma cloud or spiral MSV types (Kruskal-Wallis test, a non-parametric analog of ANOVA; $p < 0.05$). Similarly, when a cross-seasonal comparison is made (transition: April, October; winter: June, August), no significant differences in vortex duration occur for either of these two dominant MSV types (Mann-Whitney U-test; $p < 0.05$). While it is still possible that between-month or between-season differences in MSV duration occur, they are not captured by the present DMSP analysis using the relatively coarse temporal sampling of the mosaics.

Analysis of the month-to-month variations in the mean speed of MSVs (Table 2) indicates no significant differences in the translation velocities of the comma cloud systems, both across the 4 months (Kruskal-Wallis; $p < 0.05$) and when aggregated into the transition and winter "seasons" (Mann-Whitney U-test; $p < 0.05$). There is, however, a significant difference in the mean speeds for these systems between August (15.1 ± 6.80 ms^{-1}: $\bar{x} \pm$ SD) and June (13.3 ± 5.53 ms^{-1}) (Mann-Whitney; $p < 0.05$). Since Northern Hemisphere studies show a generally close association between the comma cloud signature type and the occurrence of PVA maxima, these differences suggest faster mean upper-tropospheric winds at these latitudes in the late winter and early spring; at least for 1988. For the spiral MSV type, significant differences in mean speed (at the 0.95 level of significance; Kruskal-Wallis) occur between the 4 months (Table 2). To determine which means differed significantly, we used Fisher's Least Significant Difference test and, accordingly, found differences between April (14.0 ± 9.24 ms^{-1}) and August (5.1 ± 2.50 ms^{-1}). It is interesting that, unlike the situation for the comma cloud systems, the spiral MSVs travel the slowest in August. However, some caution is appropriate in the interpretation of this finding given the relatively small sample size of these systems for the month of August. Significant differences in mean speed occur for the spiral MSVs when aggregated seasonally (at 0.95 level of significance; Mann-Whitney). These involve faster mean speeds in the transition season (13.7 ± 8.66 ms^{-1}) compared with winter (9.8 ± 9.35 ms^{-1}), and which suggest important changes in the horizontal lower-level temperature gradients at these latitudes; possibly in association

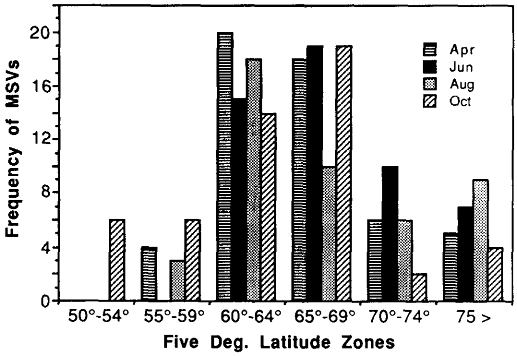

Fig. 5. MSV occurrences combined into 5° latitude zones for the months of April, June, August and October, 1988.

with the semi-annual oscillation. It remains to be seen whether these differences occur, and are in the same direction, when data for subsequent years have been analyzed.

The latitudinal variations of vortex frequency have been calculated. Fig. 5 shows that the highest frequencies of MSVs are generally in the 60–69° S zone. Latitudinal differences between months presumably result from the semi-annual oscillation in surface pressures (see also Carleton and Carpenter; 1989b, 1990).

Regions of strong horizontal thermal gradients in the low troposphere have been considered important for the formation of MSVs (Shapiro et al., 1987). Potential areas for such baroclinicity are near the sea ice-ocean margin and land ice-sea ice edge. MSVs that develop within $\pm 2.5°$ of latitude of these margins constituted about 22–43% of the total (Table 2). The highest frequencies of such cyclogenesis were in June (43%) and April (42%). It was apparently lowest in March (22%), when the extent of the sea ice is the least of any of the months studied. However, the frequencies of mesocyclones within $\pm 2.5°$ latitude of the land ice boundary were highest in March (24%), but averaged about 15% for the other months; at least in 1988. Cyclogenesis over ocean or ice surfaces had the highest frequency, averaging 49% of the total, and with March and October being 54%. The last result suggests that thermal discontinuities in the horizontal are only one of several possible factors involved in MSV development. A likely candidate for such development is the Antarctic katabatic wind regime (below).

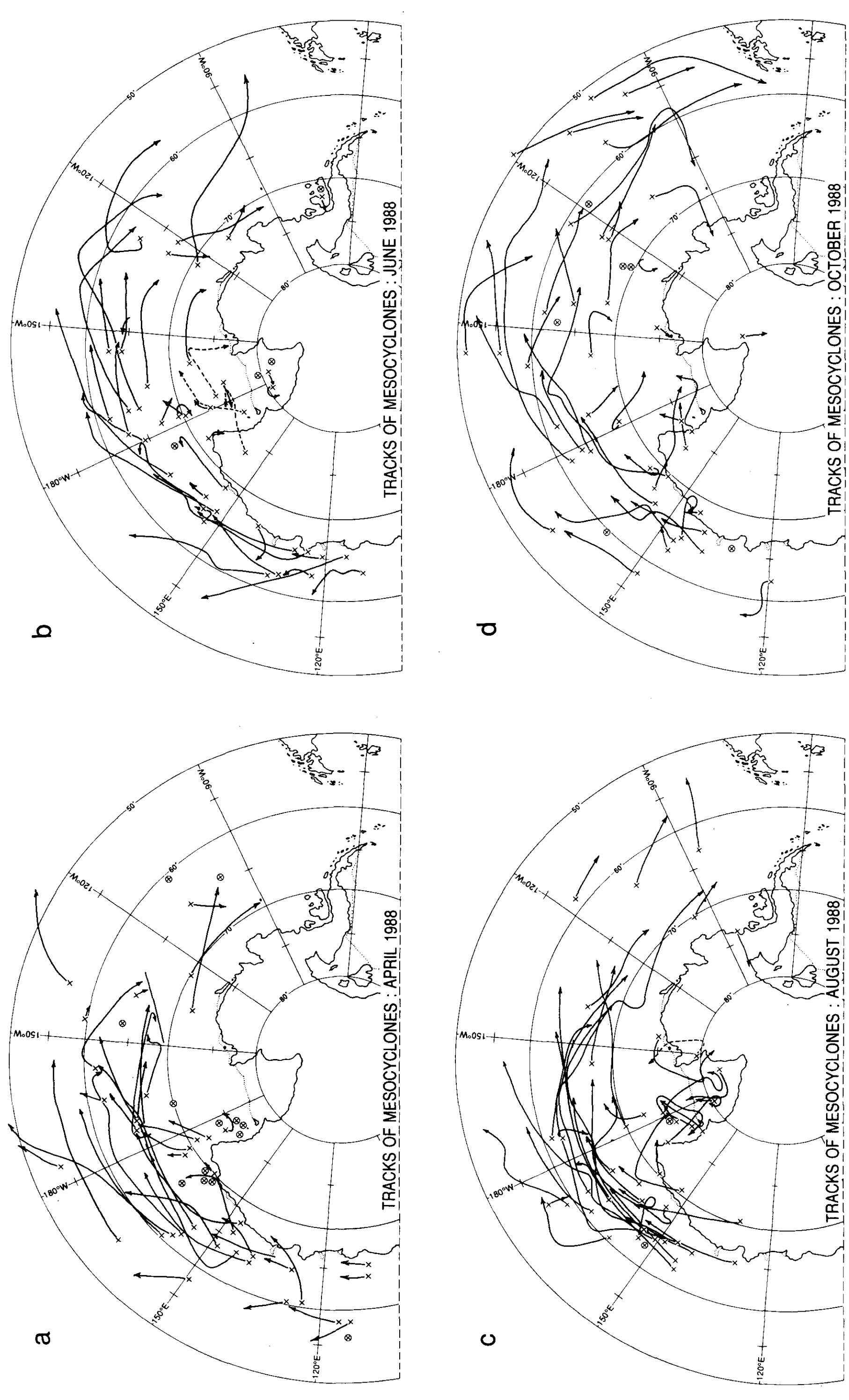

Fig. 6. (a–d) Summary maps showing tracks of MSVs identified from DMSP images: (a) April, (b) June, (c) August and (d) October, 1988. Starting points are shown by X's; end points by arrowheads. Single observation of an MSV is indicated by a circle enclosing the start "X".

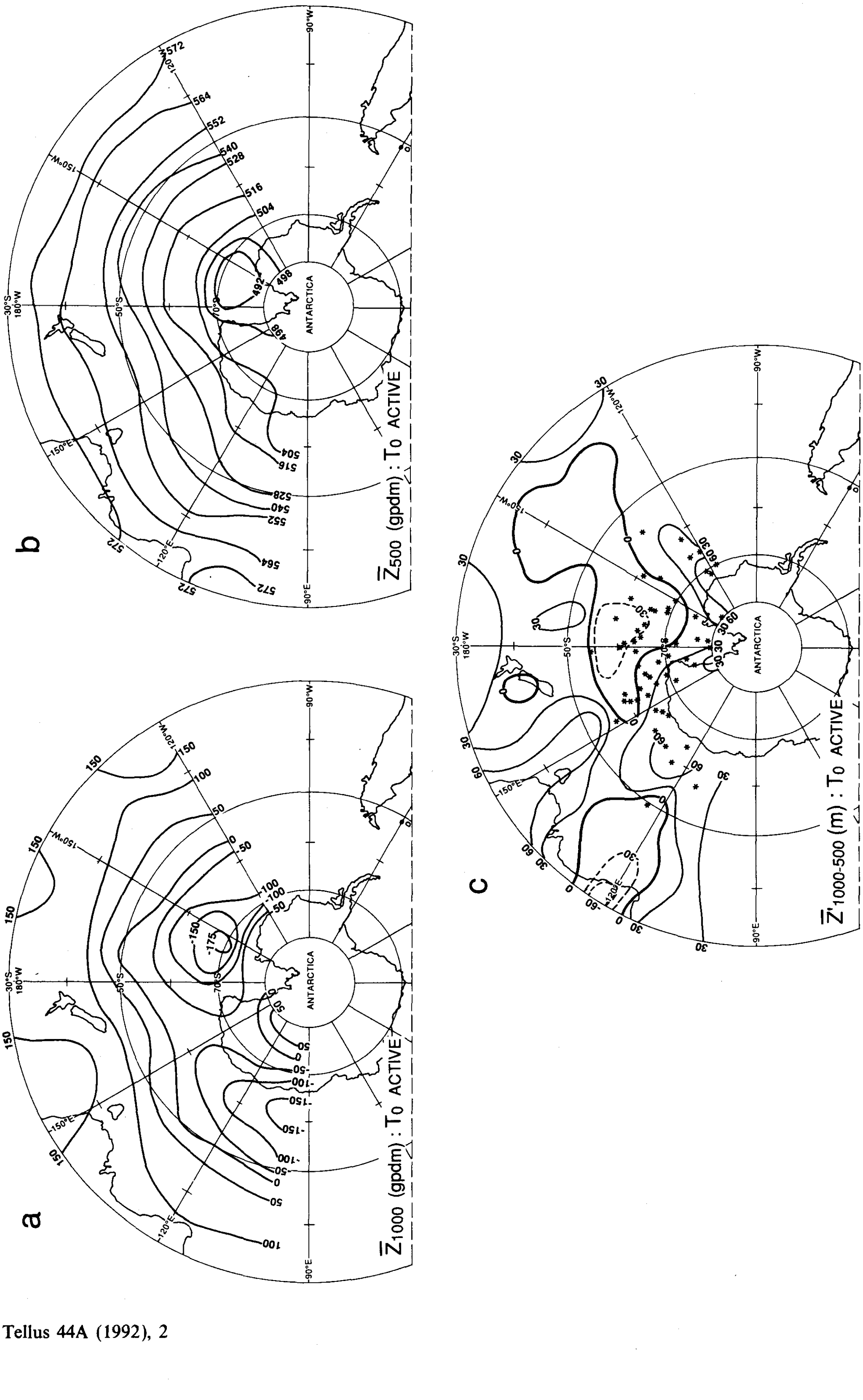

Fig. 7. (a–c) Composite anomaly maps for 11 active MSV days over the Ross Sea sector, 1988: (a) 1000 mb height, (b) 500 mb height, and (c) 1000–500 mb thickness. In (c) the locations of MSVs for these days are shown by asterisks.

Figs. 6a–d show the tracks of all Antarctic MSVs identified from the DMSP images for months having optimal TIR data coverage. Important aspects of these maps are:

(1) the net equatorward movement of MSVs, especially in the initial stages;
(2) the eastward migration of the formation areas of MSVs during 1988;
(3) the high frequencies of MSVs off East Antarctica (Marie Byrd Land) and low frequencies in the Bellinghausen Sea.

The clustering of MSVs during April (Fig. 6a) can be attribtuted to anomalous cyclonic circulations at 850 and 300 mb in the Indian and Pacific Oceans for that month (Gaffney, 1989). These anomalous wind patterns persisted through the Southern Hemisphere autumn season of 1988.

3.2. Associated broadscale circulation

The superposed epoch analysis facilitates characterization of the synoptic atmospheric conditions attending mesocyclone outbreaks. Figs. 7a–b indicate the composite 1000 and 500 mb anomaly maps for the peak (T_0) of the 11 "active" days. The negative height anomaly of 175 gpdm located at 155° W and 68° S in Fig. 7a has an associated center at 500 mb (Fig. 7b) that is displaced to the south. This suggests the role of baroclinic conditions in the outbreak of MSVs. The associated composite anomaly map for the 1000–500 mb thicknesses shows a relatively marked thermal ridge-trough pattern (Fig. 7c). These findings are broadly similar to those of Businger (1987) for MSVs in the North Pacific. MSVs dominate on the southern side of the negative (cold) thickness anomaly in Fig. 7c. They imply the significance of an enhanced thermal wind from the south and associated cold advection over the Ross Sea region for outbreaks of MSVs.

In contrast, the synoptic environments associated with the inactive MSV composite exhibit an equivalent barotropic rather than a baroclinic structure: the semi-permanent negative anomaly north of West Antarctica at the 1000 mb level is directly overlain by that at the 500 mb level (not shown). Also, there is evidence of reduced cold air outflow from Antarctica at these times. These results are further supported by the composite thickness anomaly map (Fig. 8) which shows a reduction in the temperature gradient. A distinguishing characteristic of this map (Fig. 8) is that, although the height anomalies are larger than during the active period (Fig. 7c), the ridge-trough pattern is of lower amplitude.

We tested the statistical significance of the differences between the composite heights for the active and inactive MSV groupings. Unlike

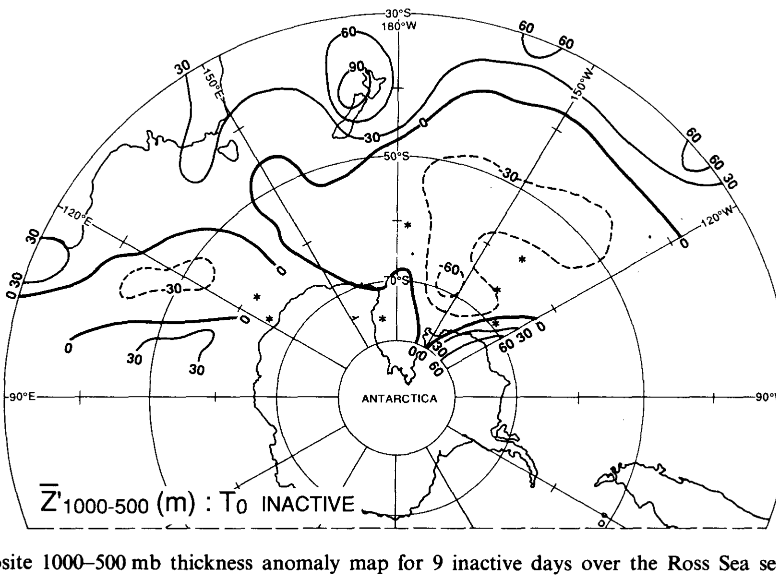

Fig. 8. Composite 1000–500 mb thickness anomaly map for 9 inactive days over the Ross Sea sector, 1988. The locations of MSVs for these days are shown by asterisks.

a recent study of MSVs in the Weddell Sea for summer conducted by Heinemann (1990), our results proved inconclusive. Only isolated points of significance were found. However, we do not feel that this invalidates our results. Our selection of "active" ("inactive") MSV days is based on peaks (troughs) in the frequency curves of MSVs for the entire sector considered (100° E eastward to 80° W). This was done in order to obtain a sufficient number of cases for the composites. However, it is possible that this approach smooths the differences in the height patterns between active and inactive periods by selecting MSVs occurring off east Antarctica as well as those in the Ross Sea sector.

Even though statistical tests were not conclusive, we have confidence in the patterns because of the broadly similar and significant results for active and inactive periods identified for the Weddell Sea by Heinemann (1990), and also for the North Pacific (Businger, 1987) and the Norwegian and Barents Seas (Ese et al., 1988).

In order to clarify further the differences between active and inactive MSV composites in terms of height and thickness anomalies, we derived longitudinal cross sections for given latitudes. The strong differences in amplitude of the waves become much more evident using this method. A pronounced ridge-trough pattern occurs for the active composite, and this is most pronounced along 60° S (Fig. 9). At 40° S, the longitudinal differences between composites are suppressed (not shown). These graphs suggest the

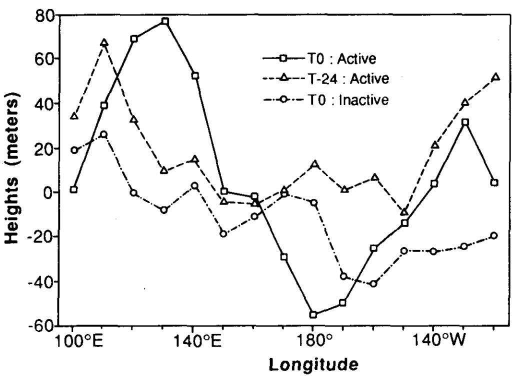

Fig. 9. Composite longitudinal thickness anomalies (meters) along 60° S: T_0, T_{-24} h for active days, and T_0 on inactive days.

importance of higher latitudes in the generation of MSV outbreaks, and the role of cold advection with an enhanced southerly thermal wind in the longitudes of the Ross Sea. There is a pronounced eastward movement of the trough-ridge pattern at 60° S, with evidence of a deepening of the trough preceding an MSV outbreak. Fig. 9 also compares the height anomaly patterns at 60° S for T_0 inactive and T_{-24} of the active MSV state. We notice a broadly similar longitudinal height pattern between these two states (T_{-24} active, T_0 inactive).

The potential role of the Antarctic katabatic wind in the onset of MSV outbreaks for the Ross Sea sector was examined using the AWS data. Due to the close proximity of many of the 29 AWS sites, 6 key stations were selected for this analysis. These are Gill, Ferrell, Jimmy, Marble Point, Whitlock and D-10 (Fig. 4). The graphs in Fig. 10a, b depict the deviations from the monthly mean temperatures for the MSV outbreak days of 11 June and 25 August 1988, respectively. These are for the time frame of T_{-72} (72 hours preceding outbreak), through T_{+48} (48 h following outbreak). At most sites, cold advection (depressed temperatures) precedes T_0 active by 24 to 48 h. Additionally, for 8 out of the 11 active days there is an out-of-phase relationship between the temperature tendencies at Gill and D-10 (e.g., Figs. 10a, b), and which may result from their location on opposing sides of the tropospheric wave (Fig. 4). We intend to pursue these suggestive findings on MSV development in subsequent research, possibly in conjunction with a mesoscale dynamical model of the Antarctic katabatic winds (e.g., Parish and Bromwich, 1986).

4. Conclusions

The "climatology" of Antarctic MSVs for the half-hemisphere centered on the Ross Sea covers the months of March, April, June, August and October of 1988. It is based on the analysis of DMSP TIR imagery that is available up to twice daily at those times, in conjunction with conventional meteorological and AWS data. There is the suggestion that MSVs may be more frequent in the transition compared with winter months. We also find, for this study period, that mesocyclones track slightly equatorward and, except for October, have a tendency to track in a latitudinally

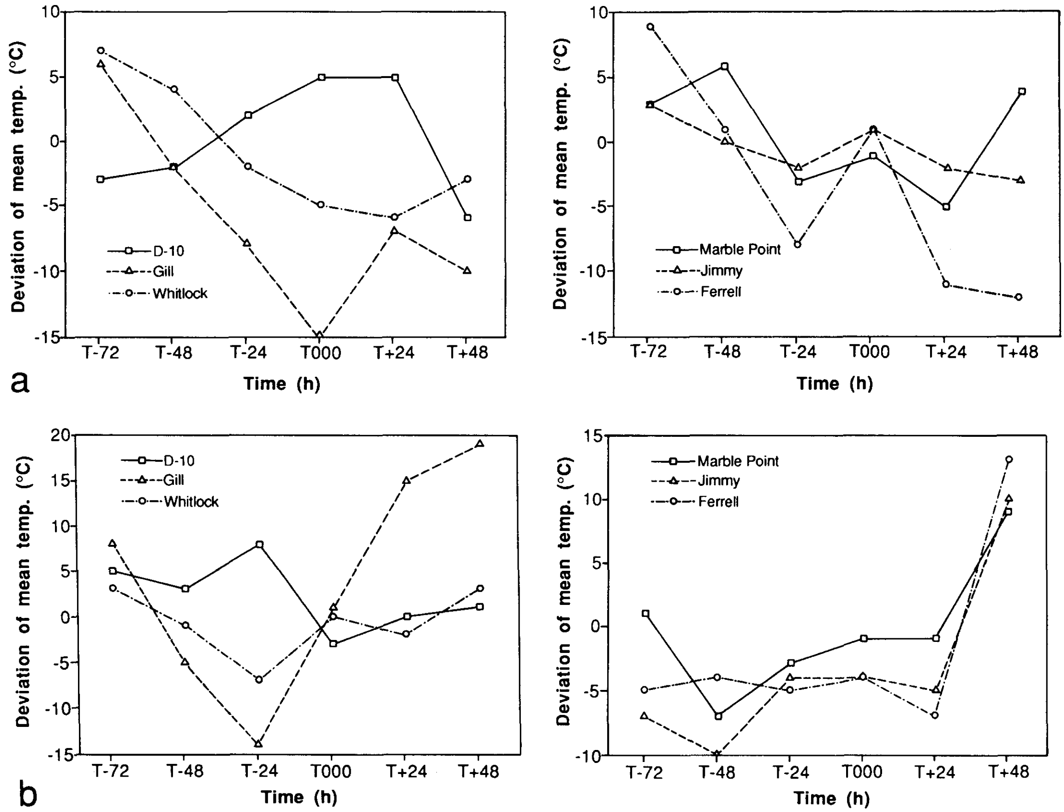

Fig. 10. Deviations from the monthly mean station temperatures for 72 h prior to through 48 h after T_0 for two MSV outbreaks. These are (a) June 11, and (b) August 25, 1988. AWS sites are Gill, Ferrell, Jimmy, Marble Point, Whitlock and D-10 (see Fig. 4 for site locations).

restricted zone. We detect a near 1:1 ratio between the "comma" and "spiral" cloud patterns for the latitudes 50–80° S. This finding contrasts with other studies that were performed on a much larger spatial scale than the present (e.g., Carleton and Carpenter, 1989a, b, 1990). Significant monthly and seasonal differences occur in the speeds of movement of the spiral signature MSVs, but not for the comma cloud systems.

The spatial distributions of MSVs during active periods show a close association with cold advection, and tend to form on the poleward side of a core of negative thickness anomalies north of the Ross Sea. The anomaly maps show enhancement of the trough northeast of the Ross Sea and the ridge in the longitudes of eastern Australia preceding active periods, and a generally baroclinic lower- to mid-troposphere. For the inactive periods the synoptic scale environment is equivalent barotropic and shows reduced amplitude of the waves. There is little evidence of a lower or middle southern latitude origin for MSVs. Rather, the formation regions, tracks of these systems, and comparisons of the longitudinal thickness anomalies at 40° S and 60° S, suggest an Antarctic source for MSV outbreaks. The AWS data tend to support the influence of the Antarctic ice sheet and katabatic outflows in the formation of MSVs, additional to the rôle of horizontal thermal gradients in marginal zones. We are in the process of performing a similar satellite-based investigation for the corresponding months of 1989 to ascertain the representativeness of our findings for this region. Those results, when available, will also facilitate an assessment of the influence, if any, of large changes in the El Niño

Southern Oscillation (ENSO) teleconnection pattern to spatial changes in the MSV regions of formation, movement and dissipation over higher southern latitudes between the two years.

5. Acknowledgements

This research was supported by NSF-DPP grant 88-16912. The published AWS data are made available on NSF-DPP grants 86-06385 and 88-18171. We are grateful to David Bromwich and Dennis Jelinski for comments and helpful suggestions at various stages of this research, and to Mike J. Hollingsworth who drafted the figures. The images were produced from USAF DMSP film transparencies archived for NOAA/NESDIS at University of Colorado, CIRES/National Snow and Ice Data Center, Campus Box 449, Boulder, CO, USA 80309. We also wish to thank the referees for their suggestions and comments, which significantly improved the presentation of this paper.

REFERENCES

Auer, Jr. A. H. 1986. An observational study of polar air depressions in the Australian region, In: Preprint volume, *Second International Conference on Southern Hemisphere Meteorology*, December 1–5, 1986. Amer. Met. Soc., Boston, Mass., 46–49.

Bromwich, D. H. 1989. Subsynoptic-scale cyclone developments in the Ross Sea sector of the Antarctic. *Polar and Arctic Lows* (eds. P. F. Twitchell, E. A. Rasmussen and K. L. Davidson). A. Deepak Publishing, 331–345, 421 pp.

Browning, K. A. and Hill, F. F. 1985. Mesoscale analysis of a polar trough interacting with a polar front. *Quart. J. Roy. Meteor. Soc. 111*, 445–432.

Businger, S. 1985. The synoptic climatology of polar low outbreaks. *Tellus 37A*, 419–432.

Businger, S. 1987. The synoptic climatology of polar low outbreaks over the Gulf of Alaska and Bering Sea. *Tellus 39A*, 307–325.

Businger, S. and Reed, R. J. 1989. Cyclogenesis in cold air masses. *Weather and Forecasting 4*, 133–156.

Carleton, A. M. 1979. The synoptic climatology of satellite-observed extratropical cyclone activity for the Southern Hemisphere winter. *Arch. Met. Geophys. Bioklim. B27*, 265–279.

Carleton, A. M. 1985. Satellite climatological aspects of the "polar low" and "instant occlusion". *Tellus 37A*, 433–450.

Carleton, A. M. and Carpenter, D. A. 1989a. Intermediate-scale sea ice-atmosphere interactions over high southern latitudes in winter. *GeoJournal 18*, 87–101.

Carleton, A. M. and Carpenter, D. A. 1989b. Satellite climatology of "polar air" vortices for the southern hemisphere winter. *Polar and Arctic Lows* (eds. P. F. Twitchell, E. A. Rasmussen and K. L. Davidson). A. Deepak Publishing, 401–413, 421 pp.

Carleton, A. M. and Carpenter, D. A. 1990. Satellite climatology of "polar lows" and broadscale climatic associations for the southern hemisphere. *Int. J. Climatol. 10*, 219–246.

Climate Monitoring Bulletin Southern Hemisphere 1988. *Bureau of Meteorology National Climate Centre.* Number 31.

Emanuel, K. A. and Rotunno, R. 1989. Polar lows as arctic hurricanes. *Tellus 41A*, 1–17.

Ese, T., Kanestrøm, I. and Pedersen, K. 1988. Climatology of polar lows over the Norwegian and Barents Seas. *Tellus 40A*, 248–255.

Forbes, G. S. and Lottes, W. D. 1985. Classification of mesoscale vortices in polar airstreams and the influence of the large-scale environment on their evolutions. *Tellus 37A*, 132–155.

Gaffney, D. 1989. Seasonal climate summary southern hemisphere (autumn 1988): ending of the equatorial Pacific warm episode (1986–87) and indications of a transitional phase. *Aust. Met. Mag. 37*, 123–128.

Harrold, T. W. and Browning, K. A. 1969. The polar low as a baroclinic disturbance. *Quart. J. Roy. Meteor. Soc. 95*, 710–723.

Heinemann, G. 1990. Mesoscale vortices in the Weddell Sea region (Antarctica). *Mon. Wea. Rev. 118*, 779–793.

Keller, L. M., Weidner, G. A., Stearns, C. R. and Sievers, M. F. 1989. *Antarctic automatic weather station data for the calendar year 1988.* Madison, WI: Department of Meteorology, University of Wisconsin.

Lyons, S. W. 1983. Characteristics of intense Antarctic depressions near the Drake Passage, In: Preprint volume, *First International Conference on Southern Hemisphere Meteorology*, July 31–August 6, 1983. Amer. Met. Soc., Boston, Mass., pp. 238–240.

Mills, B. T. and Walsh, J. E. 1988. A winter mesocyclone over the midwestern United States. *Weather and Forecasting 3*, 230–242.

Monteverdi, J. P. 1976. The single air mass disturbance and precipitation characteristics at San Francisco. *Mon. Wea. Rev. 104*, 1289–1296.

Mullen, S. L. 1979. An investigation of small synoptic-scale cyclones in polar air streams. *Mon. Wea. Rev. 107*, 1664–1647.

Myrberg, K., Koistinen, J. and Järvenoja, S. 1990. A study of non-forecasted cyclogenesis in a polar air mass over the Baltic Sea. *Tellus 42A*, 165–173.

Økland, H. 1987. Heating by organized convection as a source of polar low intensification. *Tellus 39A*, 397–407.

Parish, T. R. and Bromwich, D. H. 1986. The inversion wind pattern over West Antarctica. *Mon. Wea. Rev. 114*, 849–860.

Parish, T. R. and Bromwich, D. H. 1987. The surface windfield over the Antarctic ice sheets. *Nature 328*, 51–54.

Rasmussen, E. 1979. The polar low as an extratropical CISK disturbance. *Quart. J. Roy. Meteor. Soc. 105*, 531–549.

Rasmussen, E. 1981. An investigation of a polar low with a spiral cloud structure. *J. Atmos. Sci. 38*, 1785–1792.

Rasmussen, E. 1985. A case study of polar low development over the Barents Sea. *Tellus 37A*, 407–418.

Rasmussen, E. and Lystad, M. 1987. The Norwegian Polar Lows Project: a summary of the International Conference on Polar Lows, 20–23 May 1986, Oslo, Norway. *Bull. Amer. Met. Soc. 68*, 801–816.

Reed, R. J. 1979. Cyclogenesis in polar air streams. *Mon. Wea. Rev. 107*, 38–52.

Sardie, J. M. and Warner, T. T. 1985. A numerical study of the development mechanisms of polar lows. *Tellus 37A*, 460–477.

Schwerdtfeger, W. 1960. The seasonal variation of the strength of the southern circumpolar vortex. *Mon. Wea. Rev. 88*, 203–208.

Shapiro, M. A., Fedor, L. S. and Hampel, T. 1987. Research aircraft measurements of a polar low over the Norwegian Sea. *Tellus 39A*, 272–306.

Sinclair, M. R. 1986. Investigation of polar air stream cyclogenesis in the New Zealand area using quasi-Lagrangian diagnostics, In: Preprint volume, *Second International Conference on Southern Hemisphere Meteorology*, December 1–5, 1986. Amer. Met. Soc., Boston, Mass., pp. 50–51.

Streten, N. A. and Troup, A. J. 1973. A synoptic climatology of satellite observed cloud vortices over the Southern Hemisphere. *Quart. J. Roy. Meteor. Soc. 99*, 56–72.

Taljaard, J. J., Van Loon, H., Crutcher, H. L. and Jenne, R. L. 1969. Climate of the upper air. Part I Southern hemisphere. Vol. I US Navy NAVAIR 50-IC-55.

Wilhelmsen, K. 1985. Climatological study of gale-producing polar lows near Norway. *Tellus 37A*, 451–459.

Yarnal, B. and Henderson, K. G. 1989a. A climatology of polar low cyclogenetic regions over the North Pacific Ocean. *J. of Climate 9*, 551–566.

Yarnal, B. and Henderson, K. G. 1989b. A satellite-derived climatology of polar-low evolution in the North Pacific. *Int. J. Climatol. 2*, 1476–1491.

Zick, C. 1983. Method and results of an analysis of comma cloud development by means of vorticity fields from upper tropospheric satellite wind data. *Meteorol. Rundsch. 36*, 69–84.

Printed in Belgium